Surface Trap and Carrier Transport of Aged and Pristine Oil-paper under Harmonic Voltage by Surface Potential Decay

Shijun Li[1], Wei Yan[1], Chenyu Yan[1], Daomin Min[1], Shengtao Li[1], Wenbin Kang[2]
[1]State Key Laboratory of Electrical Insulation and Power Equipment, Xi'an Jiaotong University, Xi'an, China
[2]China Electric Power Research Insutitute, Wuhan, China

***Abstract-* Harmonic voltage can accelerate the aging of insulating materials. In this paper, an ac voltage with low-order harmonic components was applied on oil-paper insulated bushing with a duration of one month. Oil-paper samples extracted from bushing were tested by Surface Potential Decay (SPD) after positive and negative corona charging. Experimental results of SPD illustrate that the surface potential of aged oil-paper sample drops faster than the pristine one. Surface trap distribution is obtained for both pristine and aged samples. Besides, the hole and electron motilities are calculated based on transit time and initial surface potential. The conclusion can be reached that during the harmonics aging experiment, the scission of cellulose occurred under the thermal, electrical and mechanical stress, inducing surface traps and leading to higher nobilities of electron and hole.**

I. Introduction

In recent times, the power electronics and non-linear equipment can pollute the supply voltage by generating the harmonics therefore causing distortion to supply voltage. Harmonics in supply voltage was at first regarded as the indicator of partial discharge impact [1]. The presence of harmonic voltage can accelerate the aging of insulation system reducing the service life of power equipment [2-3]. Therefore, it is significant to investigate the impact of harmonics in supply voltage on dielectric properties of power equipment. Surface Potential Decay (SPD) is an effective non-destructive method to measure the surface charge profile in insulating materials. In accordance with the theoretical equations, corresponding parameters of insulating materials can be deduced such as the surface trap distribution, dc conductivity, and carrier mobility.

In this paper, an ac voltage with harmonic voltage component was applied on the oil-paper insulated bushing with a duration of one month. The oil-paper specimen was extracted directly from the bushing and tested by SPD measurement. Then, the surface trap distribution and carrier mobility of pristine and aged oil-paper samples were calculated with the help of several theoretical equations.

II. Experimental

A. Samples preparation

The 110kV oil-paper insulated bushing used in the experiment was manufactured by the Nanjing Electric (group) Co., Ltd. The harmonics aging experiment was conducted by China Electric Power Research Institute, Wuhan. As for the aging experiments parameters, according to IEC 61000-2-2, the total harmonic distortion is THD=8% or 11% with reference to long-term or short-term effects the compatibility levels respectively. However, in order to shorten the experiment duration, a remarkably high harmonic distortion (THD=20%) was chosen. Therefore, during the harmonics aging experiment, power frequency voltage (63.5kV) with 5rd harmonic voltage component (12.7kV) was applied on the bushing as shown in Fig. 1. After one-month harmonics aging experiment, the aged oil-paper specimen was extracted directly from the bushing and kept impregnated in aged oil collected from the bushing. The fresh oil-paper specimen was also prepared for control experiment. Before SPD measurement, the specimens were kept in vacuum at 90ºC for at least 12 hours to exclude the moisture. During the test, the oil-paper specimen is stuck on grounded stainless steel plate.

Fig. 1. Harmonics aging experiments of 110kV oil-paper insulated bushing

B. Experimental process

It is necessary to explain the structure and mechanism of SPD measurement system firstly. The structure of the corona discharging and SPD measurement system is explained in Fig. 2. This system is a typical needle-grid electrode system, consisting of needle electrode, mesh grid electrode and backside grounded electrode. When high voltage is applied on

978-1-5386-1194-4/17/$31.00 ©2017 IEEE

needle electrode, the electric field near the needle electrode be distorted, therefore ionizing the air and forming the positive and negative ions. Accelerated by electric field induced by mesh grid electrode, the ions will drift toward the sample, depositing on the surface and transferring traps or electrons to the surface trap states of the materials. The charges will be accumulated on the surface, and build up a surface potential. The deposited charges will traverse through the samples causing the surface potential decay. The surface potential can be captured by probe directly, which will transfer the data to computer. The Labview is applied to collect the data once a second and generate Excel sheet.

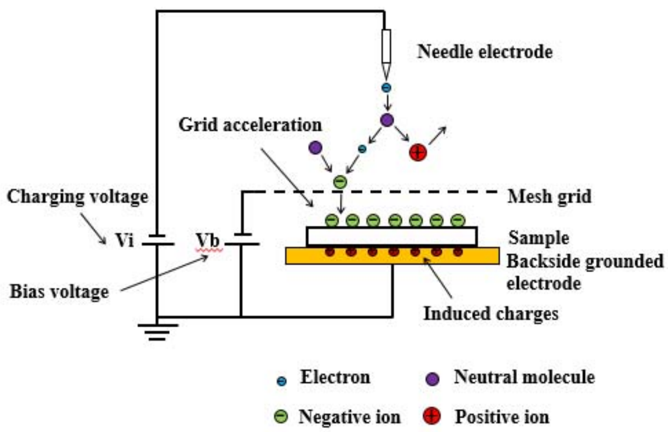

Fig. 2. Structure of SPD measurement and corona charging system

Since charge transport in insulating materials is affected by the dielectric properties of the sample and charge (type, energy) as well as atmosphere condition (temperature, humidity), the experimental condition and process for both pristine and aged specimen are well controlled as shown in TABLE I. Theoretically, the voltage of needle electrode, mesh grid and charging duration can be arbitrary as long as the voltage is high enough to ionize the air and charges can be deposited on the surface of sample.

TABLE I Experimental conditions

Parameter	Value
Sample shape (mm)	50×50×0.135
Temperature (ºC)	24-26
Humidity	30-40%
Type of charge	Positive, Negative
Voltage of needle electrode (kV)	±10
Voltage of mesh grid (kV)	±5
Charging duration (min)	1

III. Experimental Results And Analysis

A. *Experimental results*

The surface potential in oil-paper as a function of testing time under positive and negative corona charging is shown in Fig. 3.

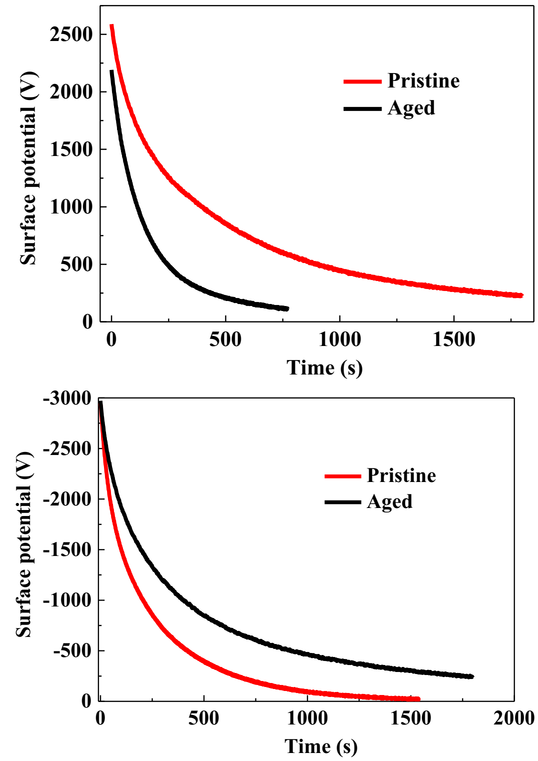

Fig. 3. Normalized surface potential as a function of testing time under positive corona charging (a) and negative corona charging (b)

According to Fig. 3, it is apparent that the surface potential of aged oil-paper specimen decays faster than the pristine ones, no matter under positive corona charging or under negative corona charging. Compared with the surface potential curve under positive charging, the one under negative charging decays more slowly. Moreover, the initial surface potential is higher under negative corona charging than that under positive corona charging.

In order to facilitate the further computation, the SPD curve can be described by double exponential decay equations as shown in Eq. (1).

$$y = y_0 + A_1 \exp\left(-x/t_1\right) + A_2 \exp\left(-x/t_2\right) \quad (1)$$

The fitting computation was conducted on Origin, and the goodness of fitting (R^2) is all over 0.99 for both pristine and aged samples under positive and negative corona charging. The corresponding parameters are shown in TABLE II.

TABLE II The simulating parameters in eq.(1)

Sample	Corona charging type	Corresponding parameters				
		$y0$	A_1	t_1	A_2	t_2
Pristine	Positive	167.1	711.3	71.5	1682.9	556.6
	Negative	-14.4	-1887.9	314.5	-1075.2	45.9
Aged	Positive	69.0	896.6	261.7	1201.8	90.4
	Negative	-159.6	-1229.4	117.6	-1861.0	1016.7

B. *Surface trap distribution*

In accordance with the surface potential decay theory, raised by Simmons, the density of surface trap as a function of trap energy is described as shown in Eq.(2). The detailed derivation of related equation was illustrated in [2], [4].

$$N_{ST}\left(E_{ST}\right)=\frac{\varepsilon_0\varepsilon_r}{elL}t\frac{\partial\phi_S\left(t\right)}{\partial t} \tag{2}$$

where N_{st} is the density of surface trap in m^{-3}, ε_0 is the vacuum permittivity equaling 8.854×10^{-12} $F\cdot m^{-1}$, ε_r is the relative permittivity constant for oil-paper, e is the elementary charge, equaling 1.602×10^{-19} C, l represents the last charged layer in m, L is the depth of the sample, t is the testing time, ϕ_s is the surface potential, E_{st} is the surface trap energy, which can be obtained by Eq.(3).

$$E_{ST}=k_BT\ln\left(\nu_{ATE}t\right) \tag{3}$$

where k_B is the Boltzmann constant, T is the testing temperature, t is the testing time, and υ_{ATE} is the attempt-to-escape frequency in s^{-1}, which can be calculated by k_BT/h, where h is the Planck constant.

The surface trap distributions for pristine and aged oil-paper under positive and negative corona charging are shown in Fig. 4.

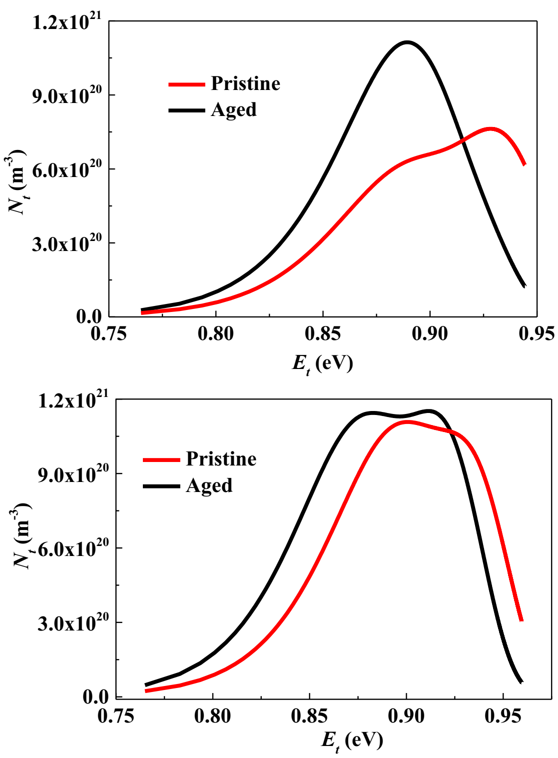

Fig. 4. Surface trap distribution under positive corona charging (a) and negative corona charging (b)

According to the calculated results, the pristine oil-paper specimen possesses two surface trap energy peaks no matter under positive charging or under negative charging. The value of surface trap energy equals 0.87-0.90eV for shallow traps and 0.93eV for deep ones. As for aged oil-paper specimen, the single energy trap for hole is observed, equaling 0.88 eV, while double energy traps for electron equaling 0.87 and 0.91eV. Besides, the surface trap density of aged oil-paper specimen is higher than that of pristine one, no matter under positive charging or under negative charging. The lower surface trap energy as well as higher shallow surface trap density leads to a greater carrier mobility for aged oil-paper specimen than that of fresh one, causing the experimental phenomenon shown in Fig. 3.

Generally, the impact of harmonics on dielectric properties of oil-paper is reflected in the fact that the density of shallow surface trap increases while the surface trap energy decrease slightly. The similar experimental results were observed in [5]. The shallow surface trap is induced by the physical defect of crystal or amorphous area in insulating materials, such as the scission in cellulose chain. The increase of shallow surface trap density indicates the generation of physical defect in oil-paper.

C. Charge carrier mobility

SPD measurement provides information about charge carrier mobility, which can be described from the initial surface potential as shown in Eq.(4). The initial surface potential is obtained directly from the SPD results.

$$-\left(\frac{d\phi_s}{dt}\right)_{t=0}=\frac{\mu}{2}\left(\frac{\phi_s}{L}\right)^2_{t=0} \tag{4}$$

where μ is the charge carrier mobility in $m^2V^{-1}s^{-1}$.
The hole and electron mobility for pristine and aged oil-paper samples calculated based on eq.(4) is listed in TABLE III.

TABLE III Hole and electron mobility for pristine and aged samples calculated based on Eq. (4)

Sample	Charge carrier	Mobility ($m^2V^{-1}s^{-1}$)
Pristine	Hole	7.15×10^{-14}
	Electron	6.21×10^{-14}
Aged	Hole	1.30×10^{-13}
	Electron	1.21×10^{-13}

Compared with the Eq.(4), another equation (Eq.(5)) was raised based on the transit time and initial potential. The detailed derivation was explained in [7-8].

$$\mu=\frac{L^2}{\phi_s t_t} \tag{5}$$

where t_t is the transit time in s, ϕ_s is the initial potential in V. The transit time is the time when the surface potential curve slope changes on log-log plot, as shown in Fig. 5. The transit times for pristine and aged samples under negative and positive corona charging are listed in TABLE IV.

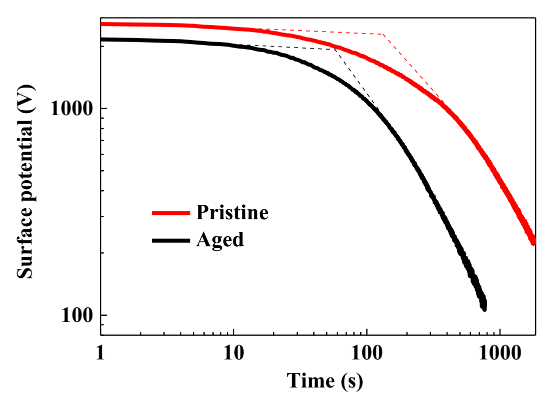

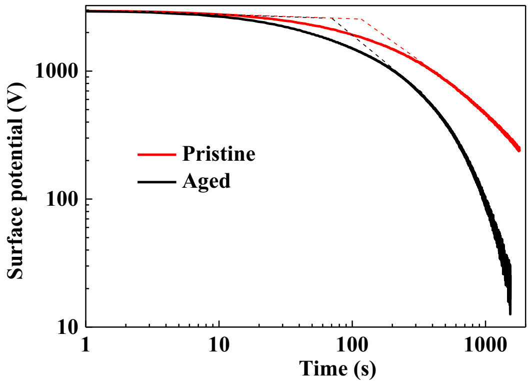

Fig. 5. Log-log plot of surface potential as a function of testing time under positive corona charging (a) and negative corona charging (b)

TABLE IV Transit time for pristine and aged samples

Sample	Charge carrier	Transit time (s)
Pristine	Hole	131
	Electron	118
Aged	Hole	57
	Electron	70

The hole and electron mobility for pristine and aged oil-paper calculated based on Eq.(5) is listed in TABLE V. Compared with the calculated results shown in TABLE III, the values are close, which means that both equations can reflect the charge carrier transport in oil-paper.

TABLE V Hole and electron mobility for pristine and aged samples calculated based on Eq. (5)

Sample	Charge carrier	Mobility ($m^2V^{-1}s^{-1}$)
Pristine	Hole	5.46×10^{-14}
	Electron	5.38×10^{-14}
Aged	Hole	1.49×10^{-13}
	Electron	8.98×10^{-14}

With regard to the comparison between hole and electron mobility, the value for hole is higher than that for electron. That's partially because the initial surface potential of samples under positive corona charging is lower than that under negative corona charging, and higher initial surface potential leads to lower mobility based on Eq.(4) and Eq.(5).

Additionally, the charge carrier mobility of aged sample is higher than that of pristine one, which further proves the phenomena that the SPD curve for aged sample drops faster than the pristine one.

IV. Conclusion

In this paper, the SPD measurement was employed to investigate the surface trap and carrier transport of aged Oil-paper under harmonics. The conclusion can be reached is listed below.

(1) The surface trap density for both electron and hole increases remarkably after harmonics aging experiment, while the surface trap energy changes slightly. That's because the scission of cellulose chain occurred during the experiment under harmonics, inducing the shallow surface traps.

(2) The electron and hole mobility for oil-paper augments after the harmonics aging experiment, which illustrates the fact that the surface potential drops faster in aged samples than in pristine ones.

Acknowledgment

This work was supported by the project of State Grid Corporation of China (No. EPRIGYKJ(2015)4268, 522722160001).

References

[1] M. Florkowski, B. Florkowska, J. Furgał and P. Zydron," Impact of High Voltage Harmonics on Interpretation of Partial Discharge Patterns", *IEEE Trans. Dielectr. Electr. Insul.*, vol. 20, No. 6, pp. 2009–2016, 2013

[2] R.Sarathi, I.P. Merin Sheema, J.Sundara Rajan, M.G. Danikas, "Influence of harmonic AC voltage on surface discharge formation in transformer insulation." *IEEE Trans. Dielect. Electr. Insul.*, vol. 5-21, pp. 2383-2393, 2014.

[3] Mazzanti G. "Reliability evaluation of insulation subjected to harmonic voltages within the limits set by international standards" *IEEE Trans. Dielect. Electr. Insul.*, vol 21- 5, pp. 2037-2046, 2014.

[4] J. Simmons, G. Taylor and M. Tam. "Thermally stimulated currents in semiconductors and insulators having arbitrary trap distributions", *Phys. Rev. B*, Vol. 7, 3714, 1973.

[5] J. Simmons and M. Tam. "Theory of isothermal currents and the direct determination of trap parameters in semiconductors and insulators containing arbitrary trap distributions", *Phys. Rev. B*, Vol. 7, 3706, 1973.

[6] Yuanxiang Zhou, Chao Dai, Meng Huang, Weijiang Chen, Fubao Jin, Jianwen Huang, "Effect of Aging Temperature on Space Charge Characteristics in Process of Thermal Aging", Vol 42, *High Voltage Engineering,* 2016 (in Chinese)

[7] T. Mizutani and M. Ieda. "Carrier transport in high-density polyethylene", *J Phys. D Appl. Phys.*, Vol. 12, 291, 1979.

[8] M. M. Perlman, T. J. Sonnonstine and J. A. St. Pierre. "Drift mobility determinations using surface‐potential decay in insulators", *J Appl. 74Phys.*, Vol. 47, 5016-5021, 1976.